



Optimising the synthesis of Birnessite



Faisal Binhudayb

Supervised by

Professor Claire Lenehan

Professor Allan Pring



8th November 2017

A thesis submitted to College of Science & Engineering of Flinders University
for the Degree of Master in Nanotechnology

DECLARATION

I declare that this dissertation is not contain any material which has been previously accepted for the award of any other degree or diploma. I also state that to the best of my knowledge and belief, no material previously published or written by another person, except where due reference is made in the thesis itself.

A handwritten signature in black ink, appearing to be 'Faisal Binhudayb', written in a cursive style.

FAISAL BINHUDAYB

8th November 2017

ACKNOWLEDGEMENTS:

I would like to take this golden opportunity to thank many people who helped and supported me throughout this year. To begin with, my sincerest thanks and appreciation goes to my supervisors, Prof. Claire Lenehan and Prof. Allan Pring, for giving me the opportunity to be a member of their group and with their support and venerated guidance made this project a real success. They encouraged me to pursue this project and welcoming me in any time for helping me to reach the desired goal without any hesitate during the project.

I sincerely thanks my parents for supporting me during my study in Australia and especially in this project as I was under pressure in some days.

I would like to thank Claire's group for their time and help during the year, particularly Jennie Bartle for the help and assistance during the project and I wish you the best with your project. Additionally, I would thank Jacqui Hull for your assistance during the research year.

The last but not least to Dr. Jason Gascooke who supported and assistance me during the year especially with SEM.

TABLE OF CONTENTS

Declaration.....	1
Acknowledgements:.....	2
Definition of Abbreviations.....	4
List of tables.....	5
List of figures.....	6
Abstract.....	7
1. Introduction.....	8
2. Aim of the project.....	15
3. Methods.....	15
3.1 General birnessite synthesis procedure.....	15
3.2 Investigations into the influence of reaction conditions.....	16
3.2.1 Reaction temperature.....	16
3.2.2 Reagent concentrations.....	16
3.2.3 Reaction pH.....	16
3.2.4 Choice of Base.....	16
3.2.5 Rate of addition of MnCl ₂	16
3.2.6 Clean-up & washing of synthesised birnessite.....	17
3.2.7 Reaction scale.....	17
3.3 Sample preparation for SEM.....	19
3.4 The parameters and the preparation for the instrumentation samples.....	19
4 Result and Discussion.....	20
4.1 Use of Potassium Hydroxide with Potassium Permanganate:.....	20
4.1.1 Reaction temperature.....	20
4.1.2 Reaction pH.....	23
4.1.3 Effect of reagent concentration.....	25
4.2 Use of sodium hydroxide with potassium permanganate:.....	27
4.2.1 Rate of addition of MnCl ₂	27
5 Conclusion.....	32
6 Future work.....	33
7 References.....	34
8 Appendix:.....	36

DEFINITION OF ABBREVIATIONS

Abbreviation	Name
DI-water	<i>De-ionised water</i>
EDXS	<i>Energy Dispersive X-ray Spectroscopy</i>
HCl	<i>Hydrochloric acid</i>
KCl	<i>Potassium chloride</i>
KOH	<i>Potassium hydroxide</i>
K-OL-1	<i>Potassium- octahedral layer material</i>
KMnO₄	<i>Potassium permanganate</i>
Mn	<i>Manganese</i>
MnCl₂	<i>Manganese chloride</i>
Mg	<i>Magnesium</i>
MnSO₄	<i>Manganese (II) sulfate</i>
(NH₄)₂CO₃	<i>Ammonium carbonate</i>
NaOH	<i>Sodium hydroxide</i>
NaMnO₄	<i>Sodium permanganate</i>
OL-1	<i>Octahedral layered</i>
Na-OL-1	<i>Sodium - octahedral layer material</i>
SEM	<i>Scanning Electron microscopy</i>
XRD	<i>X-ray Diffraction</i>

LIST OF TABLES

Table 1. Summary of the main reflections in the x-ray diffraction patterns of the major phases encountered in this study of birnessite and the symmetry and unit cell parameters for each of the phases, together with the d spacing and miller indices for each reflection.....	14
Table 2. Selected pump speed vs. flow rate delivered for a Gilson Mini plus 3 peristaltic pumps.	17
Table 3. Summary of the experimental variables tested during the synthesis of birnessite in this project.	18
Table 4. The parameters for the collection of powder x-ray diffraction pattern for the samples of the Bruker D8 powder X-ray diffractometer.....	19
Table 5. Summarised the data of X-ray diffraction for the sample that was synthesized at flow rate 1.7 ml min ⁻¹	29
Table 6. Summarised the data of X-ray diffraction for the sample that was synthesized at flow rate 0.22, 0.4 and 0.9 ml min ⁻¹	38

LIST OF FIGURES

Figure 1. Schematic diagram of the layered structure of birnessite. Layers of edge-sharing $Mn^{4+}/Mn^{3+}O_6$ are separated by layers of K^+ and Na^+ (pale-blue balls) with molecular H_2O (Lucht & Mendoza-Cortes 2015). 8

Figure 2. Schematic polyhedral representations of the crystal structures of manganese oxide minerals which have tunnel structures. All minerals can be represented by the simplified formula MnO_2 (A) pyrolusite, (B) ramsdellite, (C) hollandite, (D) romanechite and (E) todorokite. (After Post 1999). 10

Figure 3. Schematic diagram of the structure as adopted by hausmannite Mn_3O_4 and mixed Mn^{2+}/Mn^{3+} oxide 11

Figure 4. (A) amorphous structure of a glassy solid, (B) lattice structure of crystalline solid. 13

Figure 5. X-ray diffraction pattern of the synthesis of birnessite in ice-bath conditions, blue arrows related birnessite and hausmannite in red arrow. 21

Figure 6. X-ray diffraction pattern of the synthesis of birnessite at room temperature, blue arrows indicated birnessite and hausmannite in red arrow 21

Figure 7. X-ray diffraction pattern of the synthesis of birnessite at pH value of 14.7. (Blue arrows indicated birnessite). 23

Figure 8. X-ray diffraction pattern of the synthesis of birnessite after washed with KCl (blue arrows indicated birnessite and hausmannite in red). 24

Figure 9. X-ray diffraction pattern of the synthesis of birnessite by dilution of the concentration of $MnCl_2$ in 250ml of DI water. 25

Figure 10. X-ray diffraction pattern of the synthesis of birnessite by dilution of the concentration of $KMnO_4$ in 250ml of DI water. (Blue arrows indicated birnessite and hausmannite in red) 26

Figure 11. X-ray diffraction pattern of the synthesis of birnessite via $NaOH$ (1.7ml min^{-1}). (Blue arrows indicated birnessite and hausmannite in red arrows). 28

Figure 12. Manganese Pourbaix Diagram represents the stable form of manganese VS pHs (Huang 2016). 28

Figure 13. A SEM image of crystalline birnessite using sodium hydroxide 29

Figure 14. Crystalline birnessite at flow rate 1.7 ml min ⁻¹ washed with KCl(1M). Blue arrows indicated birnessite and hausmannite in red arrows.	30
Figure 15. Synthesised birnessite by using the Scaled-up Method (0.22 ml/min), blue arrows indicated birnessite and hausmannite in red arrows.	31
Figure 16. Comparison between the Scaled-up (black pattern) and down (red pattern) methods at flow rate 0.22 ml/min-1.	32

ABSTRACT

Experiments presented in this thesis explore different methods for the synthesis of birnessite with the aim of increasing the crystallite size of the resulting material. Birnessite was synthesized by reducing an alkaline solution of KMnO₄ with MnCl₂ (aq). Following this general method, various factors such as the nature of the base used, reaction temperature, the influence of pH, effect of recrystallisation with KCl, order of addition of the solutions, the rate of addition of MnCl₂ and influence of the reagent concentration were investigated. Powder XRD and SEM techniques were used to monitor the purity and particle or crystallite size of the resulting birnessite. The molar ratio of MnO₄⁻/Mn²⁺ of 0.22 was found to be the optimum ratio for synthesizing crystalline birnessite and NaOH rather than KOH was found to improve crystallite size. Room temperature and a higher value of pH, around 14.7, were found to favour synthesis of crystalline birnessite. Finally, the flow rate for the addition of MnCl₂ solution to KMnO₄ solution was optimized at a value of 0.22 ml min⁻¹.

1. INTRODUCTION

Structure and chemistry of birnessite

The main aim of this project was to explore alternative methods for the synthesis birnessite with a view to improving the crystallinity (the average crystal size), thus improving its properties as an oxidizing agent. Birnessite is a common manganese oxide mineral that occurs in a wide variety of geological environments including deep-sea nodules, crusts, surface coatings and terrestrial ore deposits (Post 1999). Furthermore, birnessite is also an important component of some soils, and it is also involved in the redox reactions and the ion exchange processes that are related to groundwater chemistry (Post 1999). Birnessite is also utilised usefully as a material for the absorption of nuclear waste from water because of its microporous properties (Shen, Ding et al. 2005). This material also has redox and ion exchange properties that make it an interesting cathode material, especially for rechargeable batteries. Birnessite is commonly recognised as a layered manganese oxide mineral (structure shown in Figure 1).

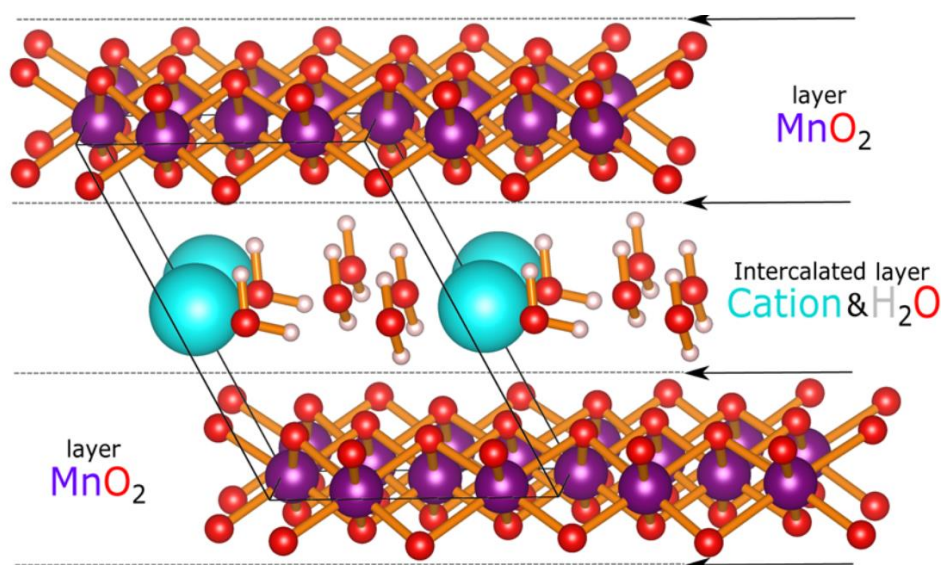


Figure 1. Schematic diagram of the layered structure of birnessite. Layers of edge-sharing $\text{Mn}^{4+}/\text{Mn}^{3+}\text{O}_6$ are separated by layers of K^+ and Na^+ (pale-blue balls) with molecular H_2O (Lucht & Mendoza-Cortes 2015).

The layers consist of edge-sharing MnO_6 octahedra with Mn existing in the Mn^{3+} and Mn^{4+} oxidation states. The interlayer region contains hydrated K, Ca and Na cations that compensate for the net negative charge on the MnO_6 octahedral layers. The spacing of the layers is about

6.9 to 7.0 Å as shown in Figure 1 (Lucht and Mendoza-Cortes 2015). Due to its layered structure, birnessite is a great precursor for the formation of pillared materials (Ta, Brugger et al. 2015). Cations such as Co and Ni are easily intercalated into the birnessite structure which results in improved thermal stabilities, good chemical actions, an increase of porosity, and possible catalytic properties.

The process of nucleation and growth of the nanoparticles has been described through the theory of the LeMar Dinegar model of burst nucleation (Baronov, Bufkin et al. 2015). Nucleation is a process in which the nuclei act as templates for the crystal growth. The homogeneous nucleation is the case of nucleation in which other crystalline matter is not present in the system. The growth of the nanoparticles is totally dependent on the two mechanisms of monomers diffusion to the surface and surface reaction. For modelling growth by diffusion the Fick's first law, Eq. 1, is applied (Chen, Jackson et al. 2016).

$$J_k = -D_K \cdot \frac{\partial C_K}{\partial X}$$

Equation 1 . Fick's first law

Where, “ J_k is the interdiffusion flux of element k, C_k is the concentration of k and D_k is the interdiffusion coefficient of element k” (Chen, Jackson et al. 2016).

Uses of birnessite

These manganese oxide minerals has been utilised for thousands and thousands of years in the past for different pigments and for clarifying glass (Negra, Ross et al. 2005). In today's world, the manganese oxide minerals are utilised as battery materials, catalysts and ores of Mn metal. More than 30 Mn of the oxide minerals are known and they occur in a large variety of the geological setting. Mn-oxide minerals are a significant part of the Mn nodules which pave huge areas of the bottoms of freshwater lakes and the ocean floors. Birnessite is a mixed valent manganese oxide, which when pillared with the transition metal oxides, result in interesting photoelectrical and electrical properties. But the variable valence compositions and states of birnessite make its industrial performance somewhat unpredictable. Thus there is a need for a method to make uniform, reproducible birnessites. OL-1 is a synthetic birnessite, which is prepared to have controllable compositions and valence states.

Manganese oxides

The complexity and variety of manganese oxide minerals are closely linked to the different possible oxidation states that Mn presents itself in nature. Manganese occurs in; +2, +3, +4 oxidation states thus giving rise to various multivalent minerals (Bobadova-Parvanova, Jackson et al. 2005). This is coupled to manganese oxides diverse atomic architecture that allows them to accommodate many metal cations. Its abundance in the Earth's crust also leads to formation of minerals in different chemical conditions and temperatures (Post 1999). The MnO_6 octahedron represents the basic building block in the majority of manganese oxide atomic structures. This leads to a variety of different structural arrangements through the different assembly of the octahedra. In essence, the structural arrangements obtained are either layer structures or tunnel structures, (also known as chain structures). Tunnel structures of manganese oxide are formed by either single, double, or triple edge sharing MnO_6 octahedra where chains share corners producing the structures that have tunnels that are either rectangular or square cross-sections. Such tunnels are filled with water molecules as well as cations, and this also extends to interlayer regions as shown in Figure 2.

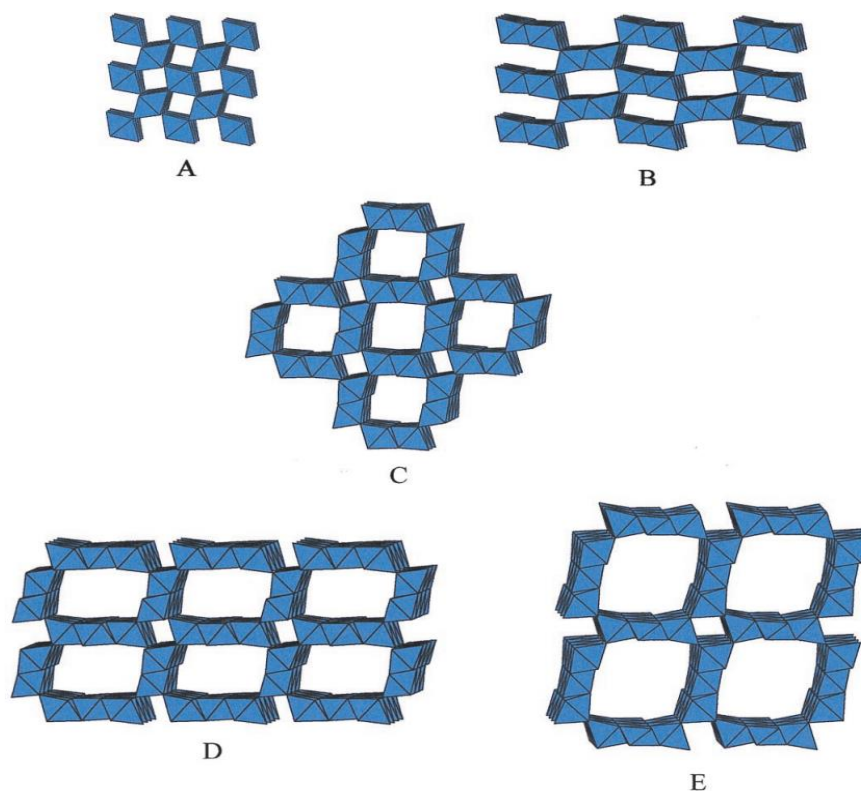


Figure 2. Schematic polyhedral representations of the crystal structures of manganese oxide minerals which have tunnel structures. All minerals can be represented by the simplified formula MnO_2 (A) pyrolusite, (B) ramsdellite, (C) hollandite, (D) romanechite and (E) todorokite. (After Post 1999).

In addition to MnO_6 octahedra, Mn also can occur in tetrahedral co-ordination and an important example of a structure with both octahedral and tetrahedral Mn coordination is the hausmannite structure (Mn_3O_4) which contains Mn^{2+} in octahedral coordination and Mn^{3+} in tetrahedral coordination. This mineral has the cubic spinel structure (figure 3).

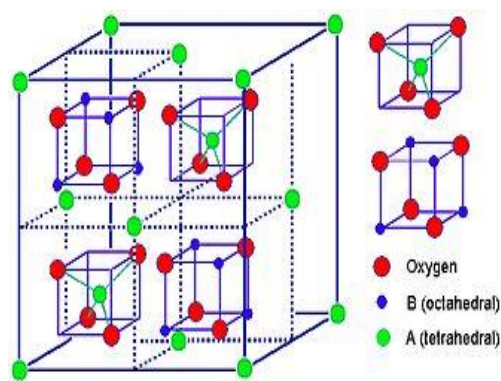


Figure 3. Schematic diagram of the spinel structure as adopted by hausmannite Mn_3O_4 and mixed Mn^{2+} Mn^{3+} oxide

Methods of birnessite synthesis

There are many different ways in which this material has been synthesized. For example passing of O_2 through the suspension of $\text{Mn}(\text{OH})_2$ which is obtained by the reactions of NaOH and Mn^{2+} for the preparation of the synthetic sodium birnessite; the hydrothermal treatment of the NaOH , MnO_2 , and the Mn_2O_3 for the production of Na-OL-1 (Octahedral layered birnessite) (Zhang, Yu et al. 2013). Furthermore, for the hydrothermal treatment of the NaMnO_4 or the KMnO_4 at $170\text{ }^\circ\text{C}$ in a slightly acidic solution for the preparation of Na or the K-OL-1, and the reaction of KOH with MnO_2 can also give K-OL-1. A second method for the production of the OL-1 are redox reactions between Mn^{2+} and permanganate in the aqueous solution which is also followed by an ageing period for the precipitate. Sol-gel processes can also be used to make birnessite, which combined with calcination can lead to OL-1. It is important to find alternate methods for the synthesis for birnessite, because many of the reported methods lack proper characterization of the product and in reality produce poorly crystalline alkali manganese oxides of uncertain structure and chemistry (Ching, Petrovay et al. 1997).

The widely used methods for the synthesis of birnessite is the oxidation of the $\text{Mn}(\text{OH})_2$ or the method of reduction of KMnO_4 which used a variety of reducing or oxidizing agents. According to McKenzie, (1971), birnessites that have low K content are very easily converted to MnO_2 or cryptomelane ($\text{KMn}_8\text{O}_{16}$) during boiling. For the reliable synthesis of birnessite it is necessary to maintain a large excess of the K^+ ions throughout the process (McKenzie 1971). In some alternative methods, the birnessite is prepared by dropwise addition of hydrochloric acid, to a boiling solution of KMnO_4 . A third method is to use the bubbled air or oxygen through the mixture of $\text{Mn}(\text{OH})_2$ and NaOH . This will give intermediate products that will have uncertain identity but can be were converted to birnessite on prolonged oxidation.

According to Post (1999), birnessite is prepared through the combination of the solution of MnCl_2 in the 2N acetic acid along with the aqueous solution of the KMnO_4 . Then these two solutions are heated to 60 °C before mixing in a beaker. The product of this mixture will be a series of birnessite containing between 0.08 to 0.25 cations of K per formula unit. The first of these three methods mentioned above will be adopted in the project without any change and the second method will be modified by the substitution of the KOH with NaOH which will lead to a more rapid oxidation to birnessite without the formation of the intermediate products. Moreover, the slightly modified third method gives cryptomelane which is a 2×2 tunnel structure. According to Negra, et al. (2005) in this method, a much more dilute suspension at the room temperature gives the same product having lower K content. In the third method, it is witnessed that cryptomelane is also a naturally occurring manganese dioxide which contains K as the essential constituent.

Characterisation of birnessite

Powder X-ray diffraction

X-ray diffraction technique is used to observe and analyse the structure of materials' at the atomic level (Raoux et al. 2007). From the diffraction pattern it is possible to obtain information on unit cell dimensions and phase identification of crystalline materials. It is important to differentiate between amorphous and crystalline birnessite because the aim of this project is to improve its crystallinity. Amorphous and crystalline solids differ in terms of its shape, cleavage and anisotropy (Figure. 4). If the birnessite is crystalline, then there should be long range order in terms of the atomic arrangement (McKenzie 1971).

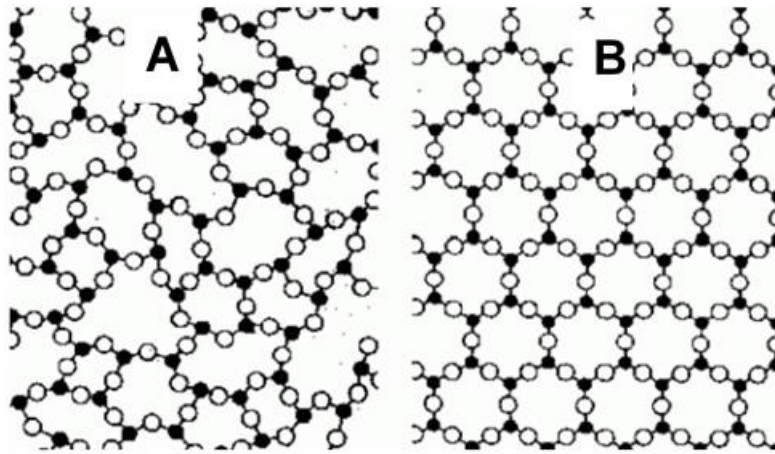


Figure 4. (A) amorphous structure of a glassy solid, (B) lattice structure of crystalline solid.

From the powder X-ray diffraction pattern it is possible to obtain a measure of the crystallite, or particle size, up to a limit of about 100 nm, due to the effects of strain in the atomic arrangement at the particle surface. Very small particles have a high surface area to volume ratio, so more of the unit cells at and near the surface are effected by strain. This leads to a broadening of the peaks or reflections in powder x-ray diffraction pattern. Using the Scherrer equation it is possible to get an approximate measure of the crystallite size.

Equation 2. Scherrer equation

$$\tau = \frac{K\lambda}{\beta \cos \theta}$$

τ is the mean size of the ordered

λ = the X-ray wavelength

β = the line broadening at half the maximum intensity (FWHM)

θ = the Bragg angle (in degrees)

To use the Scherrer equation several instrumental parameters need to be established by measuring standards. In modern powder X-ray diffractometers these instruments parameters have been established and are already embedded in a peak-width algorithm, so there is a simple function that electronically measures the peak-width and calculates the average crystallite size. There is an inverse relationship between the peak width and the crystallite size – very broad peaks are due to very small crystallite sizes (Raoux et al. 2007). Table 1 is a table of characteristic peaks for different manganese oxides.

Table 1. Summary of the main reflections in the x-ray diffraction patterns of the major phases encountered in this study of birnessite. The symmetry and unit cell parameters for each of the phases, together with the d spacing and miller indices for the major reflections.

Birnessite		Huasmannite		Potassium chloride		Cryptomelane	
monoclinic		tetragonal		cubic		tetragonal	
5.172, 2.849, 7.43 β 103.3°		5.762, 9.470		6.293		9.80, 2.870	
d (Å)	hkl	d (Å)	hkl	d (Å)	hkl	d (Å)	hkl
7.08	001	4.924	101	3.633	111	6.94	110
3.55	002	3.089	112	3.146	200	4.91	200
2.52	200	2.768	103	2.225	220	3.1	310
2.48	110	2.487	211	1.817	222	2.39	121
1.445	310	2.04	220	1.573	400	2.15	301
1.423	201					1.83	411

Scanning Electron Microscopy

Scanning Electron Microscopy (SEM) is a powerful technique for imaging the surface and morphology of fine grained materials. In addition their elemental composition can be obtained with energy dispersive X-ray (EDX) analysis, which utilizes the characteristic x-rays given off by the atoms in the sample when the electron beam interacts (Patra and Baek 2014). The solid sample is placed in the evacuated chamber, it is then exposed to a fine beam of electrons which originate in the electron gun and are focused by a series of magnetic lenses. The fine electron beam is scanned over the surface of the sample leads to a number on interactions including to the generation of both secondary and backscattered electrons (Reichelt 2007). The detector collects these electrons and converts them into the signal that displays two-dimensional images (Patra and Baek 2014). This provides information with regards to the external morphology (the sample's shape), the EDX (elemental composition), and to the crystalline structure (Reichelt 2007). In SEM imaging, the voltages for acceleration have values between 5kV and 20kV. Generally, an increase in the voltage for acceleration, leads to an increase in the resolution. However, it can lead to a decrease in the image contrast (Zhang and Zhou 2011).

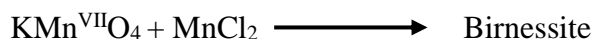
2. AIM OF THE PROJECT

The main aim of this project was to explore the influence of pH, recrystallisation with KCl, the rate of addition of MnCl₂, reaction temperature and influence of the reagent concentration on the synthesis birnessite with a view to improving the crystallinity (the average crystal size) and thus improving its properties as an oxidizing agent. In this research birnessite was synthesised from the reduction of KMnO₄ with MnCl₂.

3. METHODS

3.1 General birnessite synthesis procedure

The generic equation for the synthesis birnessite is represented by:



Equation 3. generic equation for the synthesis birnessite

The synthesis method used in this research was adapted from *Shen, Ding et al. (2005)* who synthesized birnessite by reducing an alkaline solution of KMnO₄ with MnCl_{2(aq)}. Unless otherwise specified, MnCl₂ (0.28 M, 50 mL, and 0.014 mol) was slowly added – (approximately 1-2 drops per second via a 50ml burette) to a stirred solution of basic (pH 12, 0.1 M) KMnO₄ (50 mL, 0.005 mol). The velocity of stirring was kept at mark 6 on the laboratory hot plate stirrer. The resulting precipitate was centrifuged immediately after the MnCl₂ addition was completed and the supernatant decanted. The precipitate was re-suspended in DI water to wash the product, and centrifuged, decanting the supernatant. This wash process was repeated three times. After the final wash the precipitate was collected via vacuum filtration (ADVANTEC filter paper #2) and dried in an oven at 80 °C for approximately 3 hrs.

3.2 Investigations into the influence of reaction conditions

Various factors which might have an impact on the synthesis of birnessite like the base used (KOH vs NaOH), temperature, the influence of pH, recrystallisation with KCl, order of addition of the solutions (reducant to oxidant or oxidant to reductant), the rate of addition of MnCl₂, and influence of the reagent concentration were investigated.

3.2.1 Reaction temperature

Temperature has a major influence on the synthesis and crystallization of many compounds. Some published methods require high temperatures (Turekian and Wedepohl 1961, Jenne 1968) and freezing drying processes (Crerar 1980). The reaction was performed at room temperature and in an ice-bath to see if decreasing the reaction temperature would improve the crystallinity of the resulting birnessite. In this reaction KOH was used as base medium and the other conditions were as described on pages 11 and 12 above..

3.2.2 Reagent concentrations

The influence of the reagent concentration was examined in two scenarios: by dilution of KMnO₄ (aq) and dilution of MnCl₂ (aq). For the dilute KMnO₄ reaction, KMnO₄ (250 mL, 0.005 mol) was basified with NaOH (42g) to maintain the solution pH at 14.7. All other conditions were as described in Section 0. For the dilute MnCl₂ reaction, MnCl₂ (250mL, 0.014 mol) was used. All other conditions were as described above.

3.2.3 Reaction pH

Later in the experimental program, the influence of pH of on the synthesis of birnessite was examined in two scenarios: pH 12 and also pH 14.7 of KOH. All experiment conditions that used at pH 12 were described above. The mass of KOH in this experiment was 11.241g that dissolved in 50ml of DI-water in order to adjust the pH at 14.7 and other conditions were kept as described above.

3.2.4 Choice of Base

This optimization of the synthesis utilized two different strong bases, NaOH and KOH. The appropriate mass of base was used to make the solutions pH 12 or pH 14.7.

3.2.5 Rate of addition of MnCl₂

The rate of MnCl₂ additions was examined by adding the MnCl₂ solution using a Gilson Miniplus 3 peristaltic pump. Four different pump speeds were tested. The different pump speed

provided different flow rates (Table1). In this experiment, the basic solution (pH14.7 either in KOH or NaOH) of KMnO_4 , (0.1 M, 0.005 mol) and MnCl_2 solution (0.28 M, and 0.014 mol) were prepared as described above but only 10 ml of MnCl_2 solution was added to 10 ml of the basic solution of KMnO_4 each flow rate and under various stir at 6 (magnetic bar)

Table 2. Selected pump speed vs. flow rate delivered for a Gilson Mini plus 3 peristaltic pumps.

Pump speed	Vol. delivered (ml/min)
2.5	0.22
5	0.46
10	0.9
20	1.7

3.2.6 Clean-up & washing of synthesised birnessite

The sample cleaning up was done by washing in a KCl solution that was prepared by dissolving 3.76 g of KCl in 50 ml of DI water. The resultant was washed and centrifuged immediately as described in Section 3.1.

3.2.7 Reaction scale

All the conditions that used in this experiment were used as described in Section 0. Further experiments were conducted to find out the influence of rate of addition of MnCl_2 and also recrystallise the resultant with KCl 1M.

Table 3. Summary of the experimental variables tested during the synthesis of birnessite in this project.

Parameters varied	
<ul style="list-style-type: none"> • Influence of type of bases 	<ul style="list-style-type: none"> - KOH - NaOH
<ul style="list-style-type: none"> • Thermal impact 	<ul style="list-style-type: none"> - Room temperature - Ice-bath
<ul style="list-style-type: none"> • Influence of pH of KMnO₄ solution 	<ul style="list-style-type: none"> - 12 - 14.7
<ul style="list-style-type: none"> • Rate of addition of MnCl₂ solution 	<ul style="list-style-type: none"> - 0.22 ml min⁻¹ - 0.7 ml min⁻¹ - 0.9 ml min⁻¹ - 1.7 ml min⁻¹
<ul style="list-style-type: none"> • The influence of the reagent concentration 	<ul style="list-style-type: none"> - Dilution of KMnO₄ - Dilution of MnCl₂
<ul style="list-style-type: none"> • Influence of anion 	<ul style="list-style-type: none"> - KCl
<ul style="list-style-type: none"> • Reaction scale 	<ul style="list-style-type: none"> - 10 ml of each solution - 50 ml of each solution

3.3 Sample preparation for SEM

The samples that required analysis through SEM were in powder form. The sample coated gently with a spatula on carbon tape and a stub is tapped for removing the loosely held powder. During this project, a FEI-F50 Scanning based Electron Microscopy was used with the voltages as 5 kV and 10 kV while keeping the working distance at 10 mm.

3.4 The parameters and the preparation for the instrumentation samples

The samples that required analysis through XRD were crushed into the fine powder form, by using a pestle and mortar. Thereafter, they were transformed into the slurry state on the Silicon sample disks with zero background. They were then left in order to dry them. For the XRD analysis, the Bruker D8 advanced diffractometer was utilised, which was equipped with the detector (Lynxeye XE), and the Co- X-ray tube (with λ value of 1.79 Å). Hence, the parameters shown in Table 4 were utilised.

Table 4. The parameters for the collection of powder x-ray diffraction pattern for the samples of the Bruker D8 powder X-ray diffractometer.

Parameters	Value
The X-ray Generator (Voltage in kV)	35
The X-ray Generator (current in mA)	28
Sample Rotation	10
The Value of 2 theta	10 to 90
Step size	0.15°s ⁻¹
Count time	11 min
Slit sizes	0.6mm
Filters	Fe

4 RESULT AND DISCUSSION

Initial attempts in the synthesis of birnessite were based on the reduction of alkaline (potassium hydroxide) KMnO_4 with MnCl_2 solutions. It was meant to study the influence of many parameters such as temperature, the effect of solution pH, the rate of addition of MnCl_2 , the importance of small- and large-scale variables and finally recrystallisation method that used KCl (1M) as a solvent.

4.1 Use of Potassium Hydroxide with Potassium Permanganate:

5.1.1 Reaction temperature

The first attempts were investigating the thermal effect on the synthesis of birnessite. Currently available methods for synthesis of birnessite methodologically require a high temperature (Turekian and Wedepohl 1961) and a freeze-drying process (Jenne 1968) which led to poorly crystalline birnessite. To investigate the thermal effects, the reaction was undertaken under both room temperature and ice-bath conditions, where the other conditions kept as described method. In ice-bath condition, the resulting brown precipitate was centrifuged and washed with deionized water to remove any residual ions (KCl , KMnO_4 etc) and finally analysed via powder XRD. As shown in both Figures 5 and 6, broad peaks indicated that poorly crystalline birnessite was formed in both conditions but in room temperature condition the hausmannite was found in less amount comparing to ice condition which can be seen in blue arrow. In addition, the arrows in red colour indicated the reflections from Mn_3O_4 , which

corresponds to the mineral hausmannite, appearing in XRD as a by-product under Ice-bath condition as shown in Figure 5.

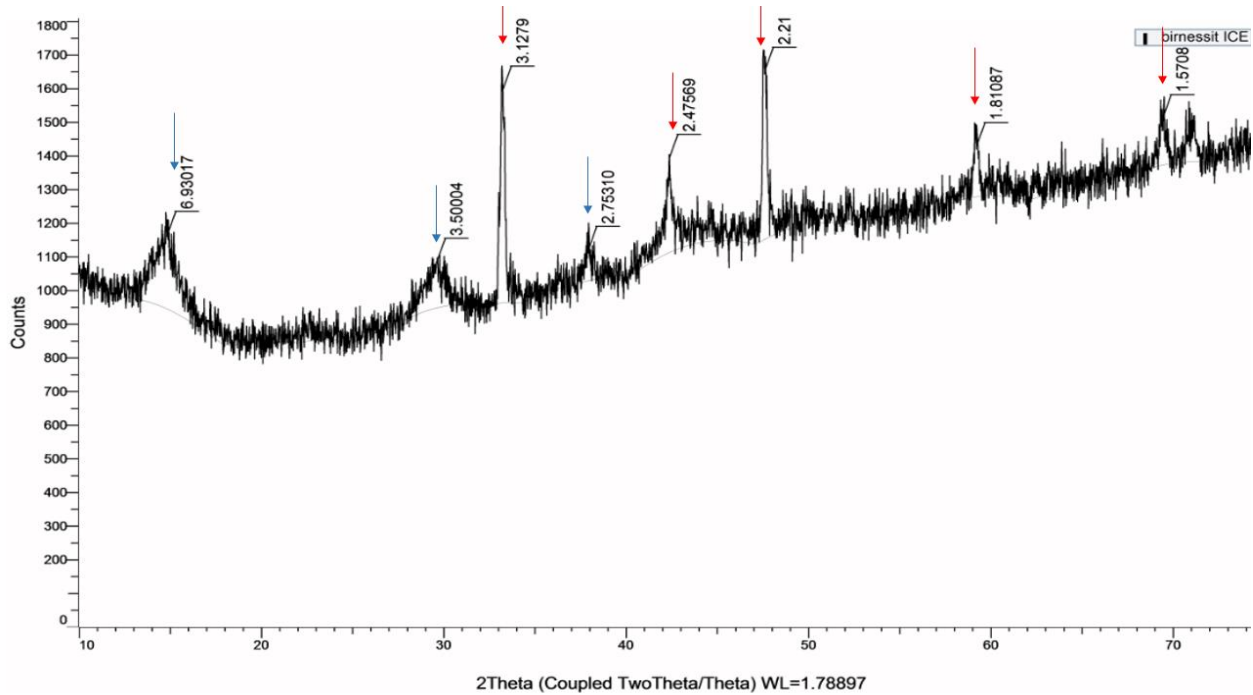


Figure 5 .X-ray diffraction pattern of the synthesis of birnessite in Ice-bath conditions, blue arrows related birnessite and hausmannite in red arrow.

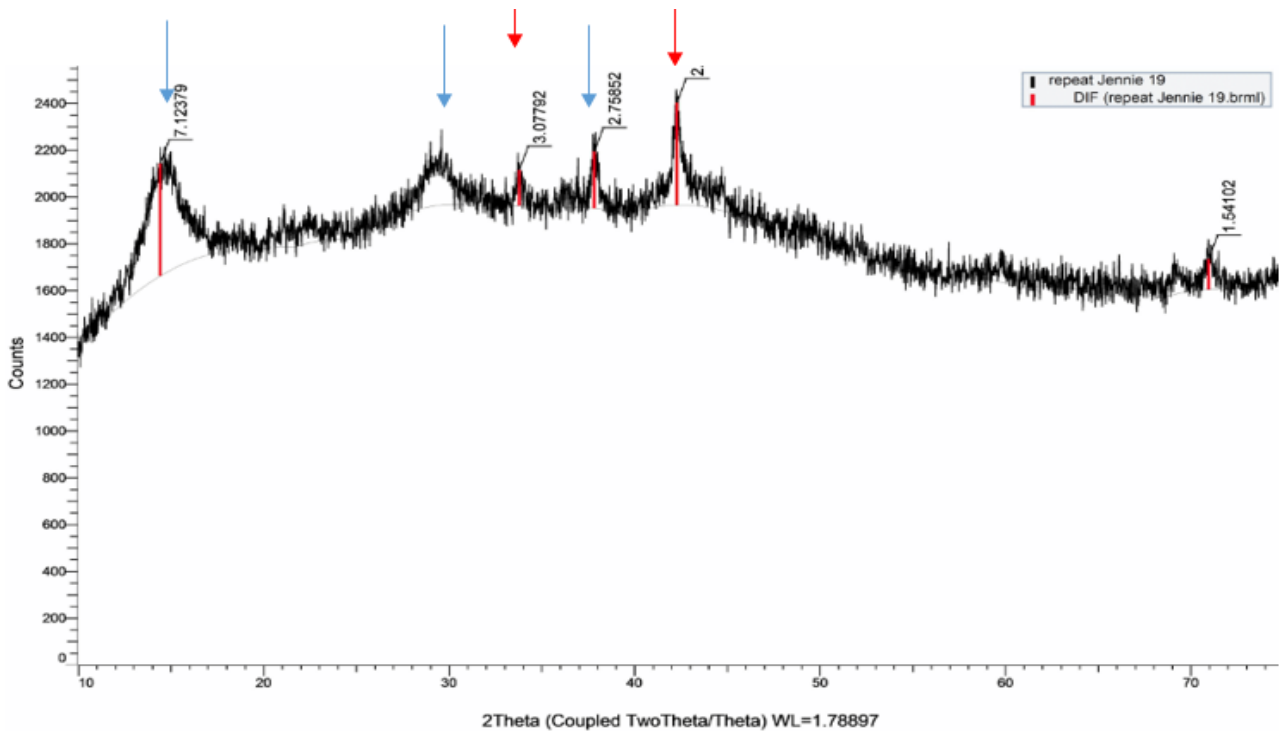
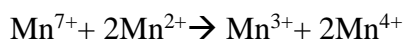
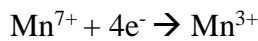


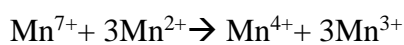
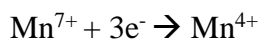
Figure 6.X-ray diffraction pattern of the synthesis of birnessite at room temperature, blue arrows indicated birnessite and hausmannite in red arrow

It is likely that, the kinetic energy is the reason behind the formation of hausmannite. Lowering the temperature will slow down the reaction and consequently reducing the kinetic energy of the complexes in solution. Therefore, the reactants will take longer to form products if given for the same concentration, resulting in formation hausmannite rather than birnessite. Consequently, a higher temperature, reduced formation of hausmannite (Boumaiza, Coustel et al. 2017). It was witnessed that the increase of reaction temperature led to a larger crystal size, better crystallinity and lower surface area of birnessite. However, the formation of hausmannite can also indicate two reactions are taking place – MnCl₂ in reducing KMnO₄ to give birnessite and also KMnO₄ is oxidizing MnCl₂ slightly to give Mn₃O₄ (hausmannite). See below

(A) Reduction of KMnO₄ into birnessite (KMn⁴⁺Mn³⁺O₄)



(B) Oxidization of MnCl₂ (Mn²⁺Mn³⁺₂O₄)



hausmannite

birnessite

4.1.2 Reaction pH

According to literature review regarding the impact of various reagents on the synthesis of birnessite many different reagents have been used like the $C_4H_4O_4$ [5], which is an organic reducing agent, NaOH, $CHNaO_2$ (Jenne 1968), $HClO_4$ (Yin, Li et al. 2014) and KOH (Boumaiza, Coustel et al. 2017) that had different values of pH. In this project, potassium hydroxide was used with pH 12 in preliminary experiments (See Figure 6) and it adjusted to 14.7 in the birnessite synthesis. Figure 6 shows that the powder XRD indicated that poorly crystalline birnessite was formed at pH 12. The powder XRD shows that birnessite was more crystalline and purer, with less hausmannite at pH 14.7 in Figure 7. It should be noted in blue that sharp peaks at $14^\circ 2\theta$, $29^\circ 2\theta$ and $42^\circ 2\theta$ and sharp crystalline peaks corresponding to d-spacings of 7.01\AA , 3.57\AA and 2.7\AA , these are consistent with the expected spacings for birnessite (Table x) and indicated that it was formed. Furthermore, peaks were corresponding to d-spacings of 4.8\AA , 3.1\AA and 2.75\AA , which were an indication of hausmannite (Mn_3O_4).

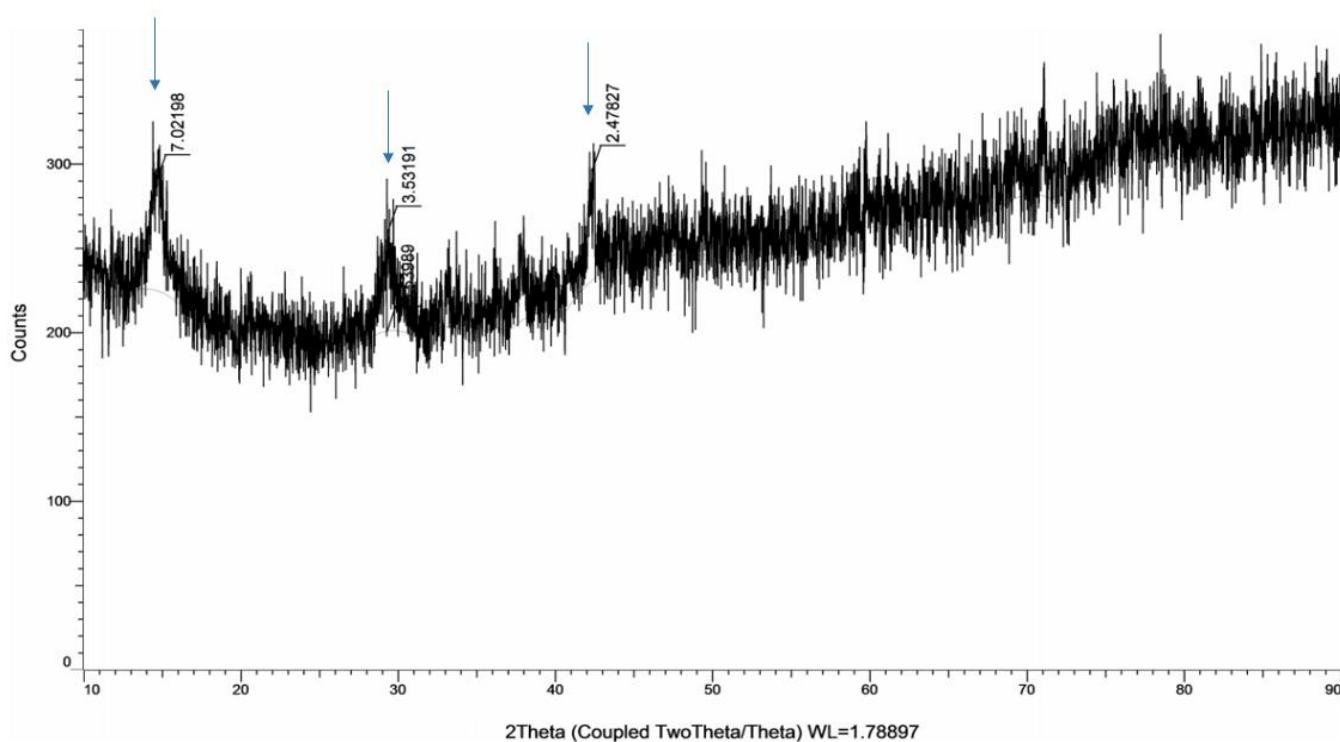


Figure 7. X-ray diffraction pattern of the synthesis of birnessite at pH value of 14.7. (Blue arrows indicated birnessite).

A subsequent experiment where for both samples were recrystallized with KCl (1 mol L⁻¹). The XRD peaks or reflections were sharper with less peak broadening, which indicated that the birnessite was more coarsely crystalline but still contained Mn₃O₄ Figure 8.

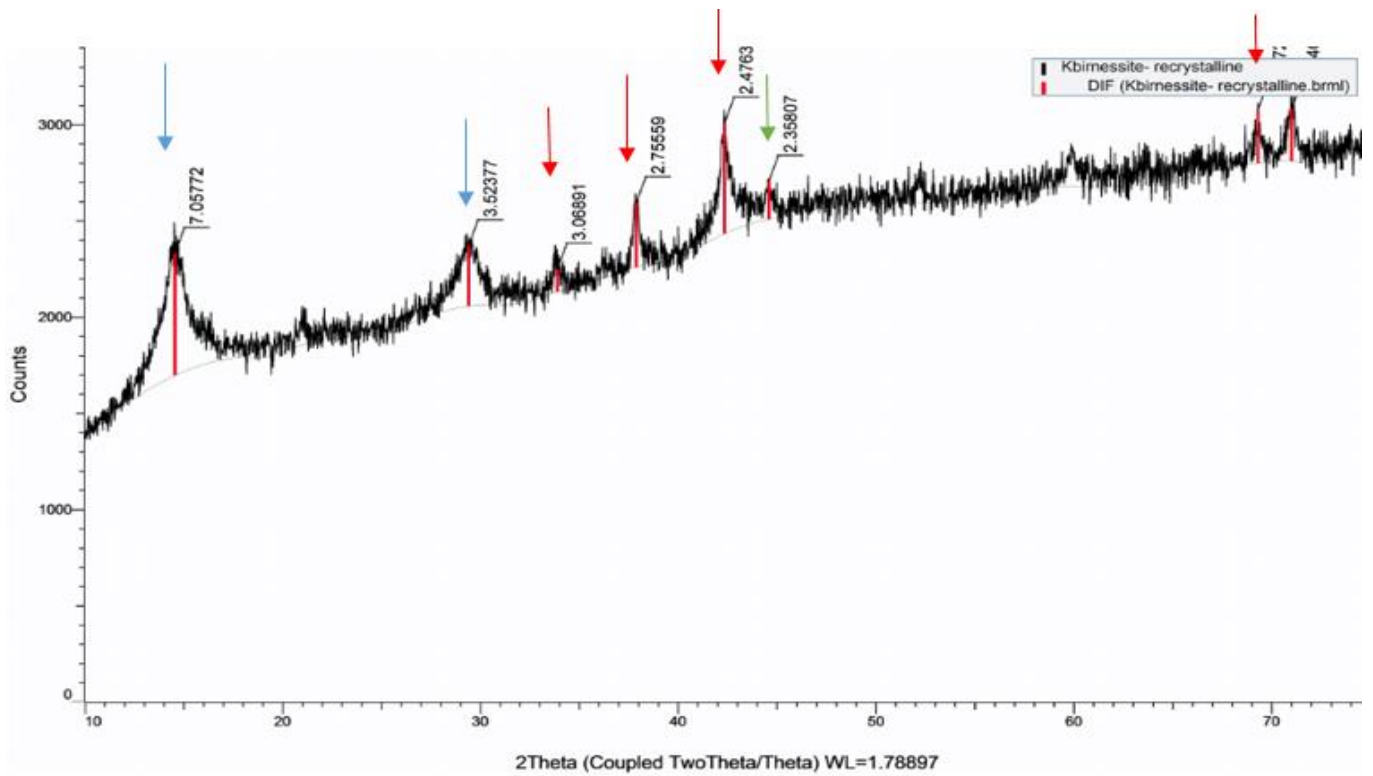
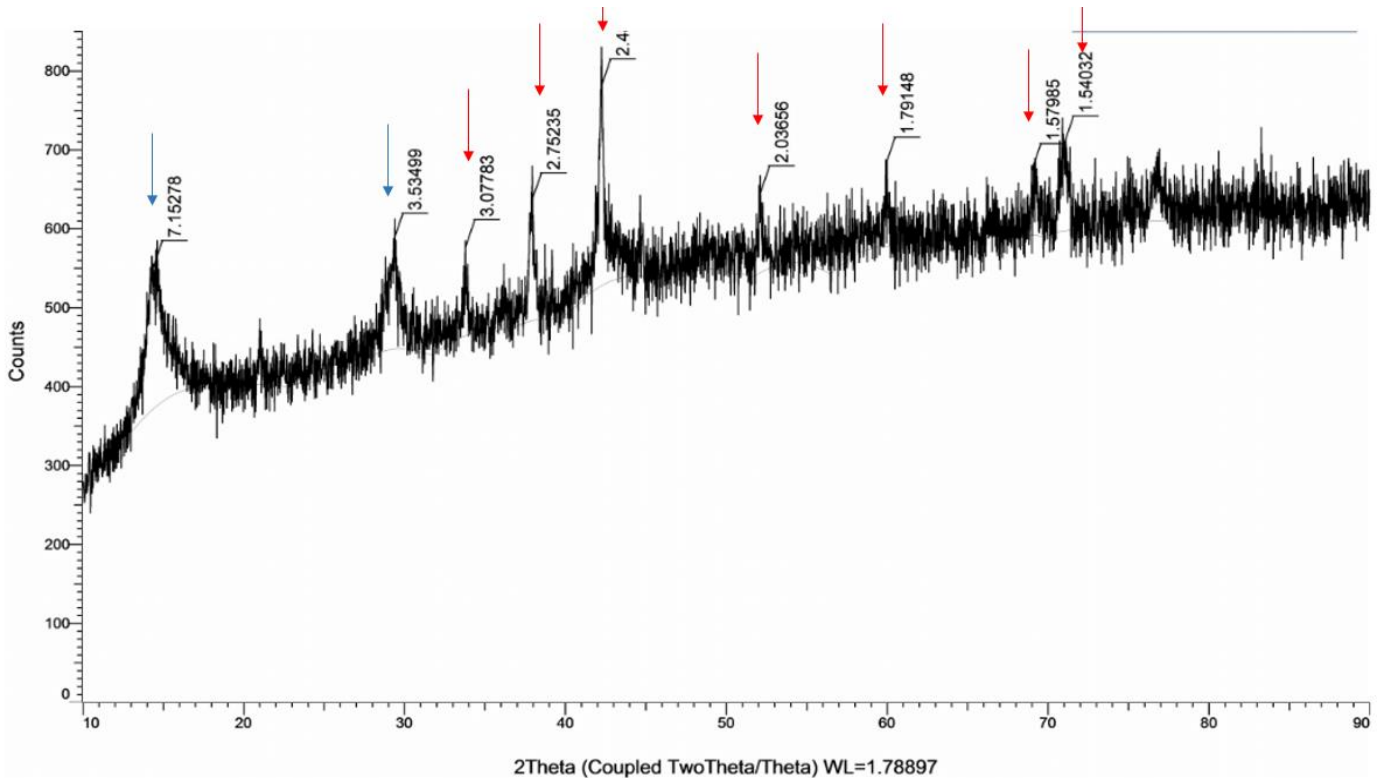


Figure 8. X-ray diffraction pattern of the synthesis of birnessite after washed with KCl (blue arrows indicated birnessite and hausmannite in red).

4.1.3 Effect of reagent concentration

The effect of reagent concentration in the second reaction was based on diluting the concentration of one of the reagents. In the first experiments the basic of $KMnO_4$ in 250ml of DI water while the concentration of $MnCl_2$ was kept constant in 50 ml of DI water. Also, the concentration of $MnCl_2$ was diluted in 250 ml of DI water and the level of $KMnO_4$ was kept constant in 50 ml. Figure 9 and 10 are shown the observation for diluting the concentration of $KMnO_4$ in 250ml of DI water and also diluting the concentration of $MnCl_2$ respectively which indicated that the manganese mineral hausmannite (Mn_3O_4) was observed and identified as it labelled in red arrows at $35^\circ 2\theta$, $38^\circ 2\theta$, $43^\circ 2\theta$ and $45^\circ 2\theta$, the birnessite also obtained in



poor crystalline form which were shown in blue arrows.(fig.10).

Figure 9.X-ray diffraction pattern of the synthesis of birnessite by dilution of the concentration of $MnCl_2$ in 250ml of DI water.

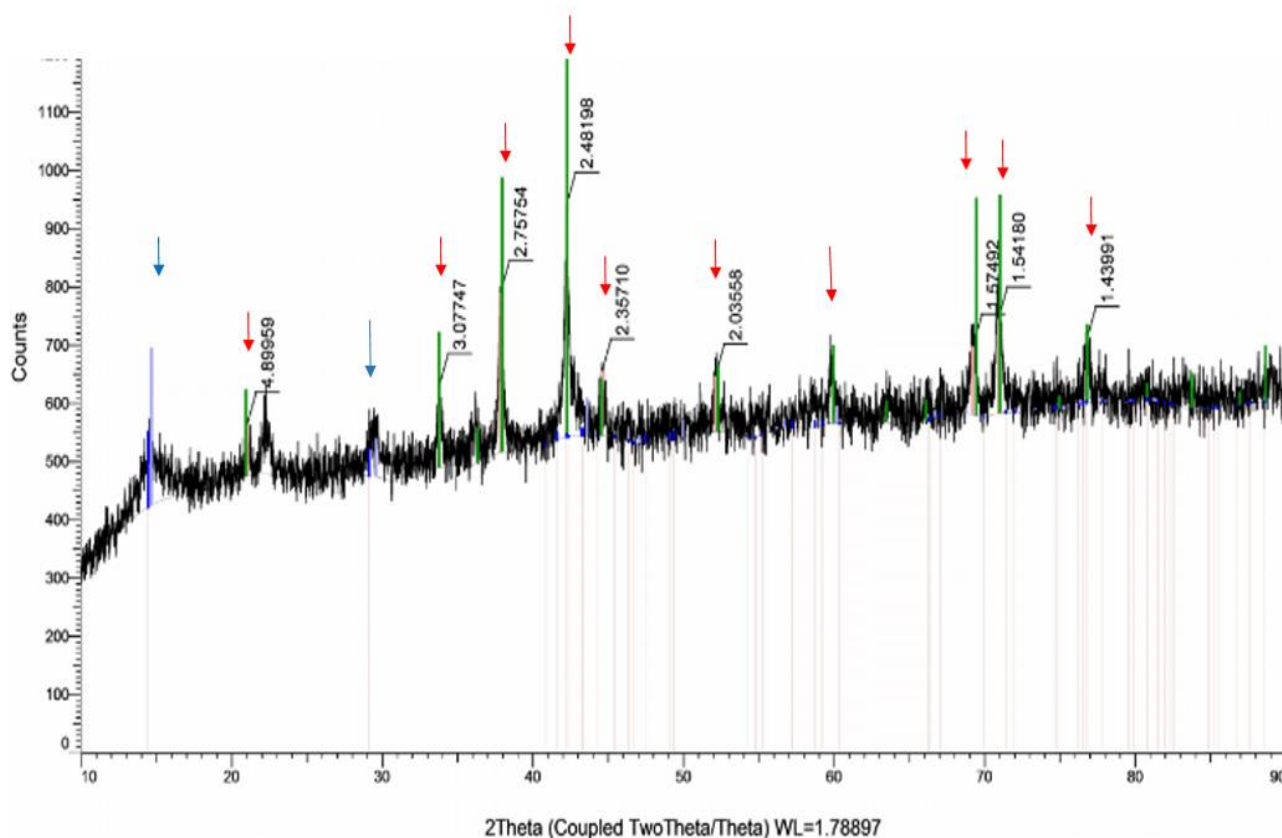


Figure 10. X-ray diffraction pattern of the synthesis of birnessite by dilution of the concentration of KMnO_4 in 250ml of DI water. (Blue arrows indicated birnessite and hausmannite in red).

A series of further experiments were undertaken to investigate the effect of rate of adding MnCl_2 in the process of synthesising crystalline birnessite. The powder XRD results can be seen in appendix file (see **Figure A1-A4**) which indicated that the rate of addition of MnCl_2 did not make any improve the crystallinity of birnessite (fig. A2). The results of these experiments are consistent with poor crystalline product. To create a highly crystalline birnessite room temperature should be considered as the kinetic energy of the molecules are higher. Moreover, the ratio $\text{MnO}^{+7}/\text{Mn}^{+2}$ of 0.22 was sufficient to oxidise the Mn. It is contrary to the study by Boumaiza, Coustel et al. (2017) that indicated that the molar ratio of 0.33 is too low and hence recommended higher molar ratio in further experiments. However, it should also be noted that crystalline birnessite can be synthesised by another strong base such as NaOH as a reagent.

4.2 Use of sodium hydroxide with potassium permanganate:

4.2.1 Rate of addition of MnCl_2

The resultant XRD patterns for the syntheses using different flow rates for addition of MnCl_2 showed sharp reflections at $14.49^\circ 2\theta$ and $29.19^\circ 2\theta$ which are corresponding to birnessite. These peaks correspond to the characteristic birnessite reflections at d-spacings 7.1 \AA and 3.5 \AA which can be seen in blue as shown figure 6. Adding Mn^{2+} to a basic solution forces the Mn^{2+} to give electrons to the Mn^{7+} to remain stable. Consequently, this electron exchange results in the formation of Mn^{4+} species that are insoluble in water and cause precipitation of the manganese which can be seen on the right side of the diagram in Figure 11 (Huang 2016). **Table 5** summarised the data of X-ray diffraction for the sample that was synthesized at flow rate 1.7 ml min^{-1} which are similar to the other rates of addition of MnCl_2 those can be found in appendix. The XRD pattern for the reaction at flow rate 1.7 ml min^{-1} summarised in Figure 10 for peaks 001 and 002, which are the main reflections for birnessite (blue arrow). The manganese mineral hausmannite (Mn_3O_4) was observed at $38^\circ 2\theta$ and $43^\circ 2\theta$, its main XRD reflections are indicated by red arrows in Figure 10. The relative height of the hausmannite reflections compare to the birnessite reflections indicate it is only present as a small peaks in this experimental product. The result was recorded and is shown in Figure 10.

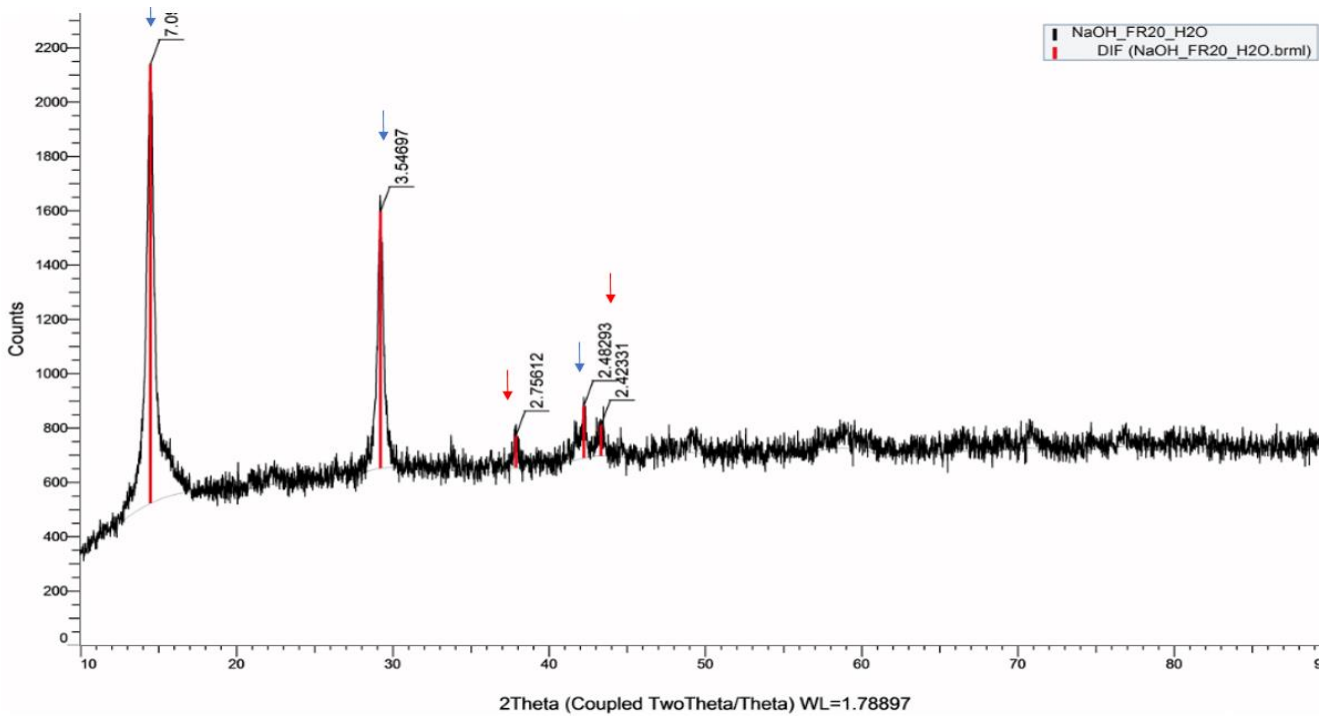


Figure 11. X-ray diffraction pattern of the synthesis of birnessite via NaOH (1.7ml min⁻¹). (Blue arrows indicated birnessite and hausmannite in red arrows).

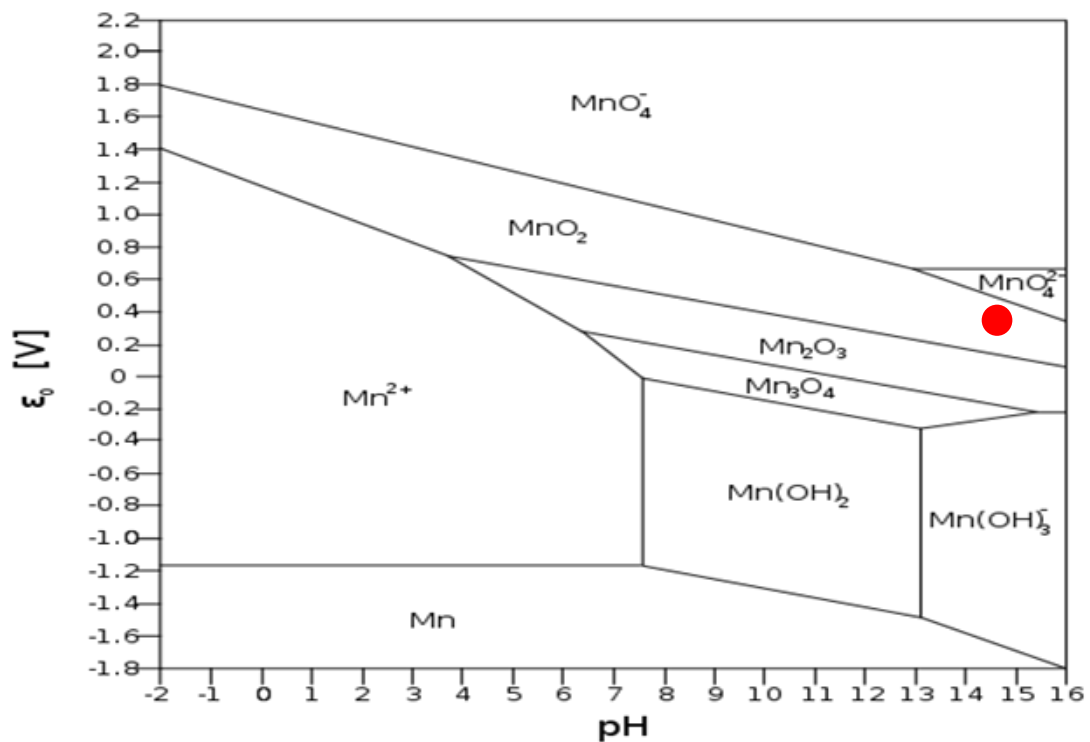


Figure 12. Manganese Pourbaix Diagram represents the stable form of manganese VS pHs (Huang 2016). The red dot point indicates the stable form of manganese for birnessite at pH 14.7.

However, low rate of addition of $MnCl_2$ (1 ml/min) did not give a positive result for the synthesis of birnessite. Also, birnessite could not be synthesised in 40 ml/min which was as the fastest rate of addition of $MnCl_2$ used in these experiments. This is in agreement with Boumaiza, Coustel et al. (2017) who suggested that the crystallinity of Birnessite depends on kinetic not thermodynamic constraints and lowering the rate of addition of an oxidant solution will decrease the amount of hausmannite (Mn_3O_4).

Table 5. Summarised the data of X-ray diffraction for the sample that was synthesized at flow rate 1.7 ml min⁻¹.

1.7 ml/min	Position (θ)	Size (nm)	d-spacing(\AA)
Peak 1	14.499	27.52	7.094
Peak 2	29.196	29.82	3.552

SEM conducted on a crystalline birnessite using sodium hydroxide to control the pH is shown in Figure 12. The formation of small platelets is an indication that layered birnessite structure was formed, as anticipated, due to the crystalline nature of the sample

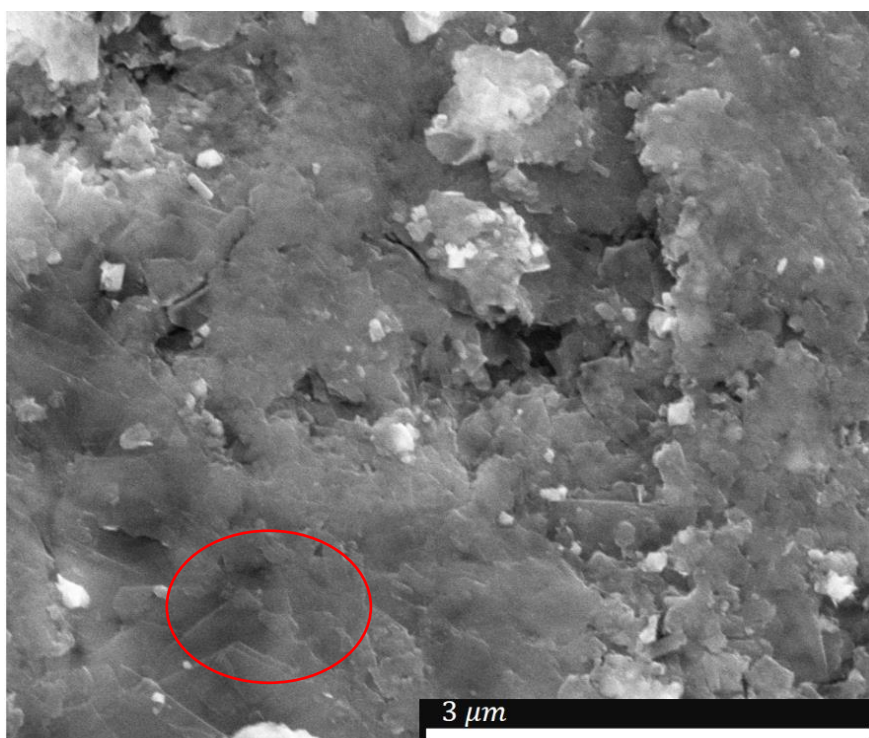


Figure 13.A SEM image of crystalline birnessite using sodium hydroxide. The red circle highlights the crystalline birnessite (platelet form).

The effects of salt on the synthesis of crystalline birnessite using potassium chloride were investigated. The resultant precipitate was washed and centrifuged with DI-water and lastly dried at 80°C. Observing the XRD pattern, minimal changes in the size of the particle were noted, which the average size for the reflections (001) at 2θ 14.355° and (002) at 2θ 29.372° after recrystallization step was 18.08 nm whereas the average size before the recrystallization step was 24.165 nm in the same position (Figure 13), indicating larger crystals. Also, the lack of sharp crystalline peaks with corresponding d-spacings of 2.757 Å and 2.458 Å formed which indicates the manganese mineral hausmannite (Mn_3O_4) may dissolved.

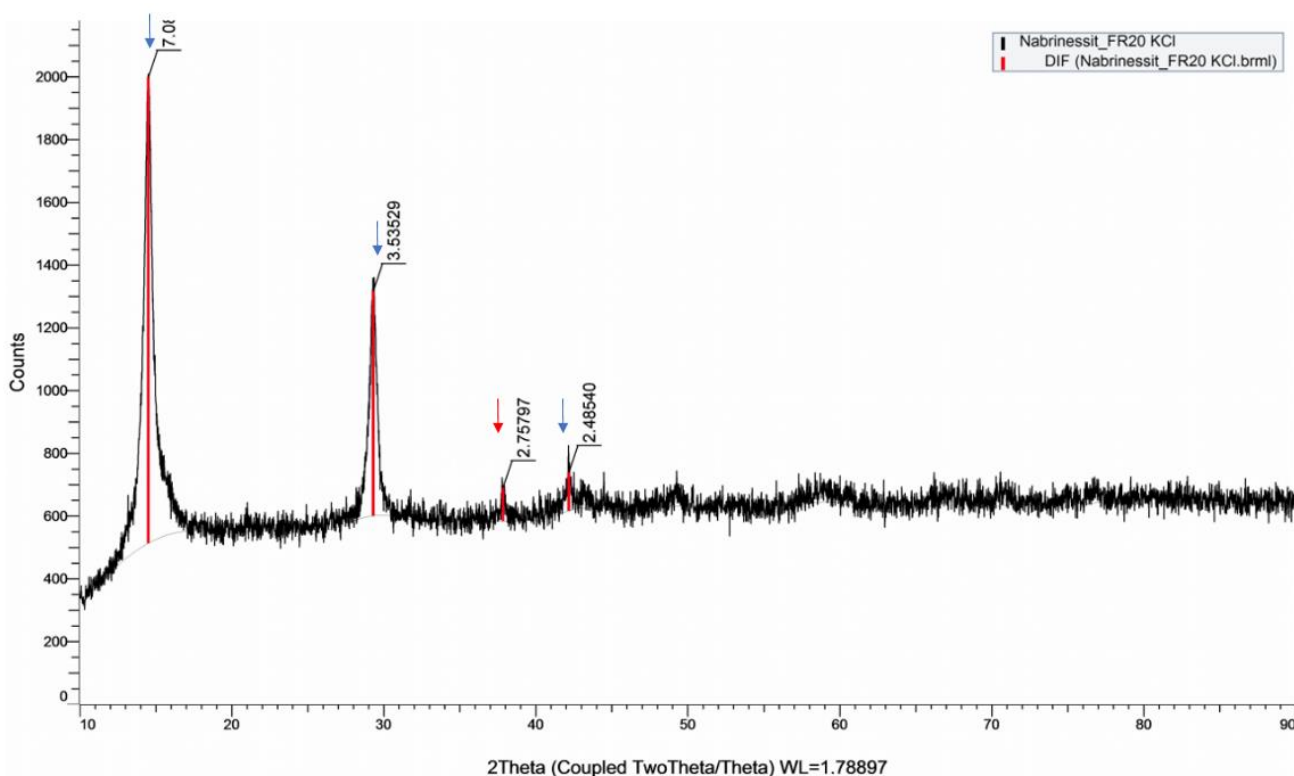


Figure 14. Crystalline birnessite at flow rate 1.7 ml min⁻¹ washed with KCl(1M). Blue arrows indicated birnessite and hausmannite in red arrows.

It's clear from the sharpness of the reflections in the powder x-ray diffraction pattern that there is a significant improvement in the crystallite size. This indicates that the birnessite has been recrystallised or the crystallites have grown in size. It is important to note that this procedure results in the disappearance of the powder lines for hausmannite. It is possible that there are two methods by which the crystallinity of birnessite is improved by stirring with a KCl solution. Stirring in KCl solution may dissolve hausmannite and the Mn^{+2} and Mn^{+3} from

this phase are now in solution. It is also possible that during this process the birnessite also dissolves and reprecipitates growing larger birnessite crystal.

The alternative explanation is that the manganese released from the dissolution of hausmannite is oxidised in solution by contact with the atmosphere and grows on birnessite on the existing birnessite crystallites, thus resulting in longer birnessite crystals. To test these hypotheses one could see if coarsening occurs if the process is repeated in the absence of air.

A scaled-up method was attempted with the employment of the reduction of KMnO_4 with MnCl_2 in the presence of sodium hydroxide as a strong base medium. Further experiments were conducted to find out the influence of rate of addition of MnCl_2 and also recrystallise the resultant with KCl (1M). The XRD pattern indicated that the crystalline birnessite was obtained only when the flow rate is 0.22 ml min^{-1} (Figure.14).

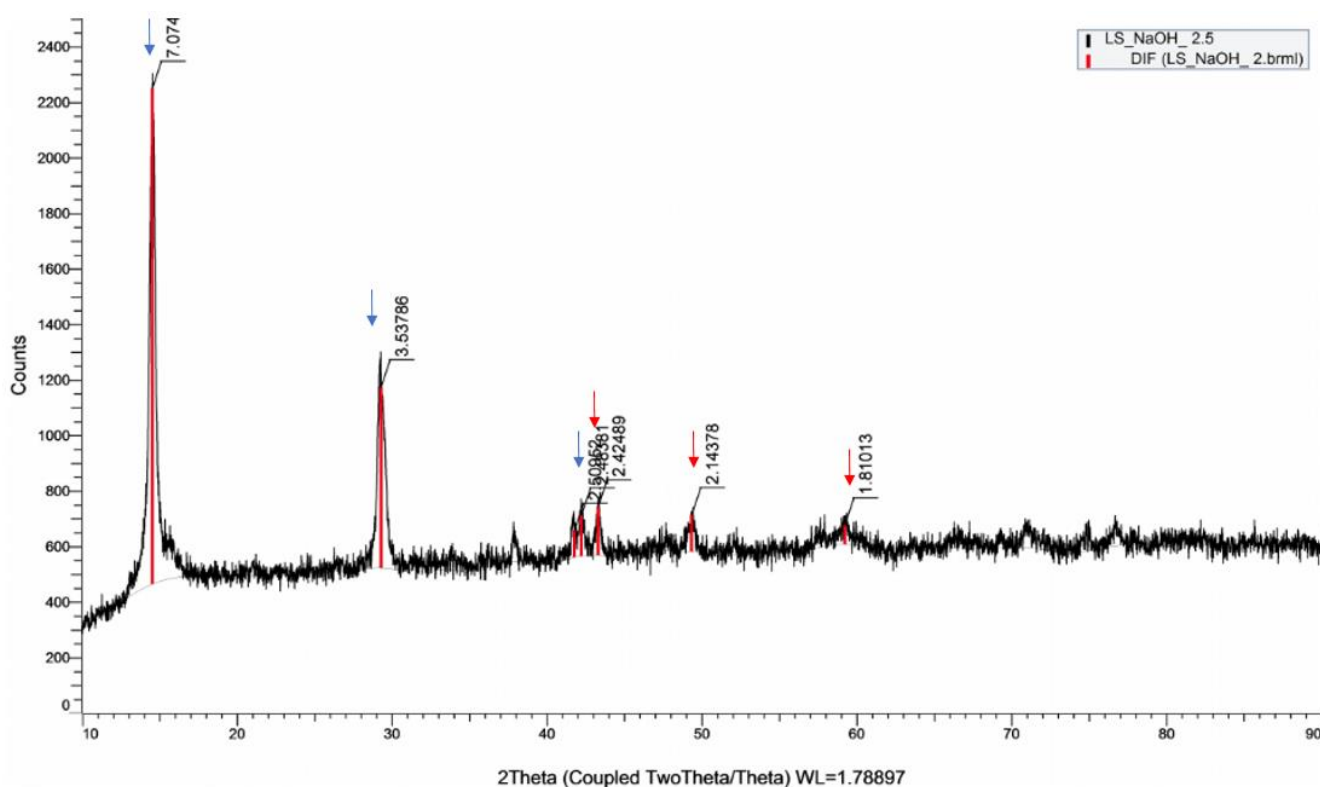


Figure 15. Synthesised birnessite by using the Scaled-up Method (0.22 ml/min), blue arrows indicated birnessite and hausmannite in red arrows.

Additionally, **Figure 15** showed the comparison between the two methods for synthesising crystalline birnessite which was scaled up and down in the same flow rate (0.22 ml min^{-1}). Therefore it should be noted that it was found out that the rate of adding MnCl_2 was a

determinant in the synthesis of birnessite and its consequent crystallisation. Moreover, room temperature was also found to be ideal in harvesting highly crystalline birnessite (Wu et al.,2016).

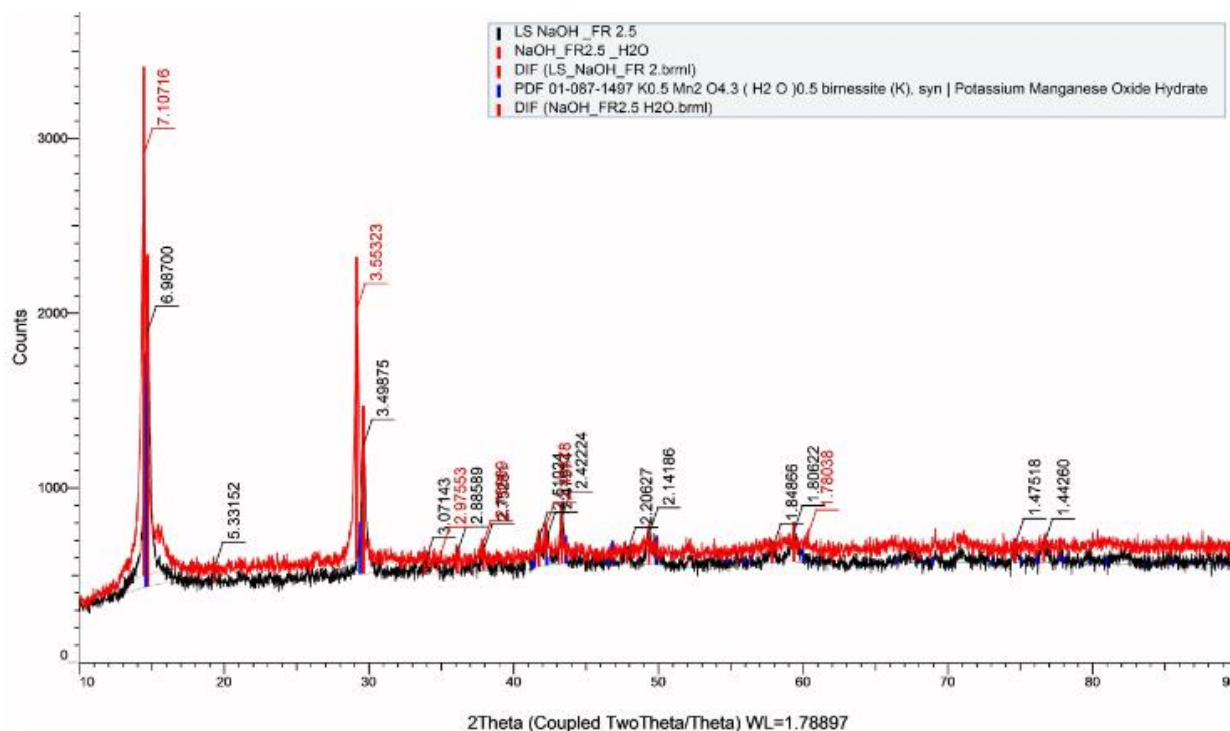


Figure 16. Comparison between the Scaled-up (black pattern) and down (red pattern) methods at flow rate 0.22 ml/min-1.

5 CONCLUSION

In this project the crystallite size of birnessite was increased by recrystallization using a solution of KCl. The techniques of powder XRD and SEM have been used in the experiment for monitoring the crystallization and morphology of birnessite. This was produced from the oxidation of $MnCl_2$ by $KMnO_4$ in the NaOH solution. Moreover, the crystallization of birnessite also got influenced by the variation in the molar ratio of MnO_4^-/Mn^{2+} and other factors like the temperature, recrystallize with KCl, the rate of addition of $MnCl_2$, influence of the reagent concentration and the influence of pH impact on the synthesis of birnessite. The optimized conditions for synthesizing crystalline birnessite were based on the molar ratio of MnO_4^-/Mn^{2+} which was 0.22 and also the NaOH was preferred to synthesis birnessite instead of KOH. Additionally, room temperature was also found to be ideal in harvesting highly

crystalline birnessite as well as higher value of pH(14.7). The flow rate of MnCl_2 at 0.22 ml min^{-1} was to the optimized flow rate to synthesis birnessite in scaled up and down versions.

6 FUTURE WORK

Even though there has been extensive research on the synthesis of birnessite as can be gauged by the large number of journal articles on this topic and the variety of possible methods for the synthesis birnessite. The current research reported above indicates a number of factors are important in the synthesis of birnessite. For example, use of NaOH instead of KOH is important in the synthesis high crystalline of birnessite. It is also important to consider magnesium, aluminium and zinc as reducing agents in the synthesis of birnessite instead of any other reducing agent in future research. The use of sodium permanganate rather than potassium permanganate should be investigated as a starting material with those reagents and studying the influence of rate of addition of MnCl_2 , temperature, etc . Also, studying the influence of the other salts, such as KBr on the crystallinity of birnessite could be investigated.

7 REFERENCES

- Baronov, A., et al. (2015). "A simple model of burst nucleation." Physical Chemistry Chemical Physics **17**(32): 20846-20852.
- Bobadova-Parvanova, P., et al. (2005). "Structure, bonding, and magnetism in manganese clusters." The Journal of chemical physics **122**(1): 014310.
- Boumaiza, H., et al. (2017). "Conditions for the formation of pure birnessite during the oxidation of Mn (II) cations in aqueous alkaline medium." Journal of Solid State Chemistry **248**: 18-25.
- Chen, H., et al. (2016). "Modelling and experimental study on β -phase depletion behaviour of HVOF sprayed free-standing CoNiCrAlY coatings during oxidation." Surface and Coatings Technology **291**: 34-42.
- Ching, S., et al. (1997). "Sol- Gel Synthesis of Layered Birnessite-Type Manganese Oxides." Inorganic Chemistry **36**(5): 883-890.
- Crerar, D. A., Cormick, R K and Barnes, H L, (1980). "in Geology and Geochemistry of Manganese, eds. Varentsov, I. M. & Grasselly, Gy. ." E. Schweizerbart'sche Verlagsbuchhandlung, Stuttgart **1**: 293-334.
- Huang, H.-H. (2016). "The Eh-pH Diagram and Its Advances." Metals **6**(1): 23.
- Jenne, E. A. (1968). Controls on Mn, Fe, Co, Ni, Cu, and Zn concentrations in soils and water: the significant role of hydrous Mn and Fe oxides, ACS Publications.
- Lucht, K. P. and J. L. Mendoza-Cortes (2015). "Birnessite: a layered manganese oxide to capture sunlight for water-splitting catalysis." The Journal of Physical Chemistry C **119**(40): 22838-22846.
- McKenzie, R. (1971). "The synthesis of birnessite, cryptomelane, and some other oxides and hydroxides of manganese." Mineralogical Magazine **38**(296): 493-502.
- Negra, C., et al. (2005). "Soil manganese oxides and trace metals." Soil Science Society of America Journal **69**(2): 353-361.
- Park, S., et al. (2009). "Measuring the crystallinity index of cellulose by solid state ^{13}C nuclear magnetic resonance." Cellulose **16**(4): 641-647.
- Patra, J. K. and K.-H. Baek (2014). "Green nanobiotechnology: factors affecting synthesis and characterization techniques." Journal of Nanomaterials **2014**: 219.
- Post, J. E. (1999). "Manganese oxide minerals: Crystal structures and economic and environmental significance." Proceedings of the National Academy of Sciences **96**(7): 3447-3454.
- Raoux, S., et al. (2007). X-ray diffraction studies of the crystallization of phase change nanoparticles produced by self-assembly-based techniques. Proc. Europ. Symp. On Phase Change and Ovonic Science.
- Reichelt, R. (2007). Scanning electron microscopy. Science of microscopy, Springer: 133-272.

Shen, X. F., et al. (2005). "Control of Nanometer-Scale Tunnel Sizes of Porous Manganese Oxide Octahedral Molecular Sieve Nanomaterials." Advanced Materials **17**(7): 805-809.

Speakman, S. A. (2011). "Basics of X-ray powder diffraction." Massachusetts-USA, 2011a. Disponível em:<
<http://prism.mit.edu/xray/Basics%20of%20X-Ray%20Powder%20Diffraction.pdf>.

Ta, C., et al. (2015). "Effect of manganese oxide minerals and complexes on gold mobilization and speciation." Chemical Geology **407**: 10-20.

Turekian, K. K. and K. H. Wedepohl (1961). "Distribution of the elements in some major units of the earth's crust." Geological Society of America Bulletin **72**(2): 175-192.

Yin, H., et al. (2014). "Effects of Co and Ni co-doping on the structure and reactivity of hexagonal birnessite." Chemical Geology **381**: 10-20.

Zhang, X., et al. (2013). "Rapid hydrothermal synthesis of hierarchical nanostructures assembled from ultrathin birnessite-type MnO₂ nanosheets for supercapacitor applications." Electrochimica Acta **89**: 523-529.

Zhang, X. and Z. H. Zhou (2011). "Limiting factors in atomic resolution cryo electron microscopy: no simple tricks." Journal of structural biology **175**(3): 253-263.

8 APPENDIX:

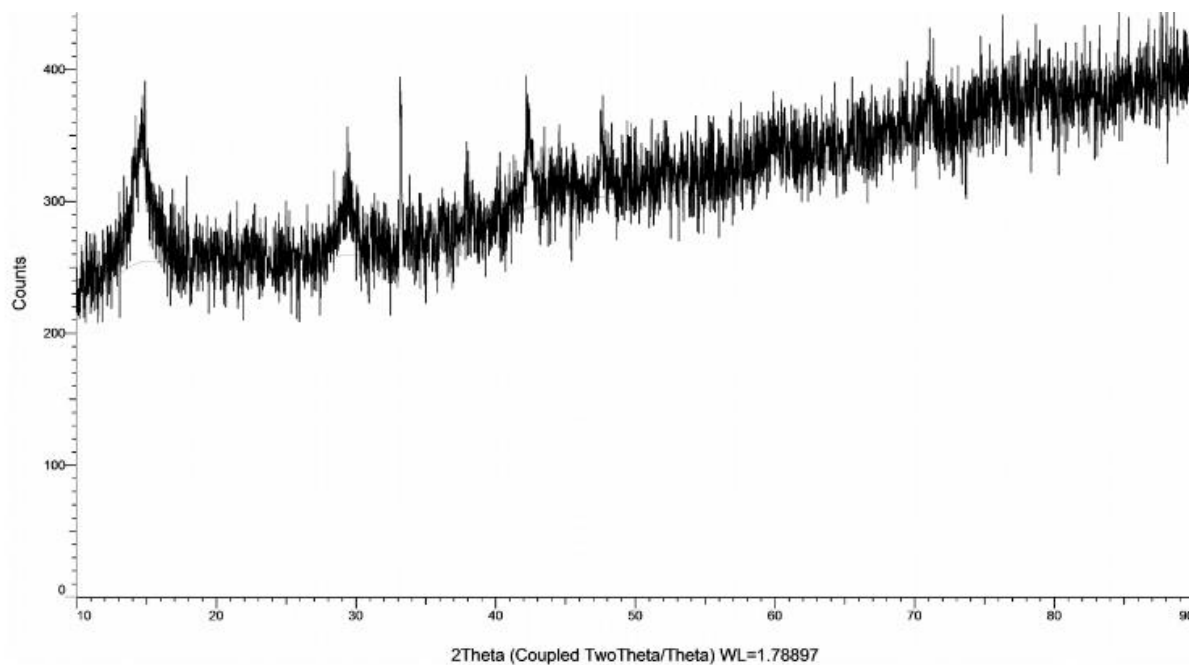


Figure A1. X-ray diffraction pattern of the synthesis of birnessite via KOH (0.22ml min^{-1})

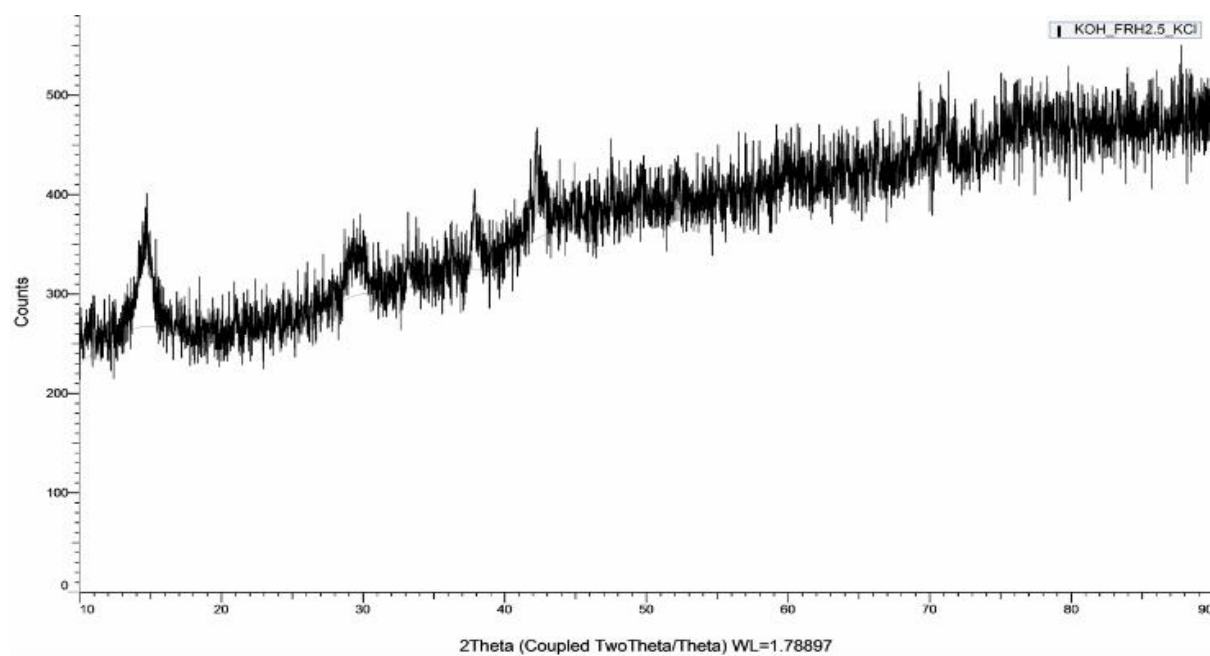


Figure A2. X-ray diffraction pattern of the synthesis of birnessite via KOH (0.22ml min^{-1}) after washed with KCl 1M.

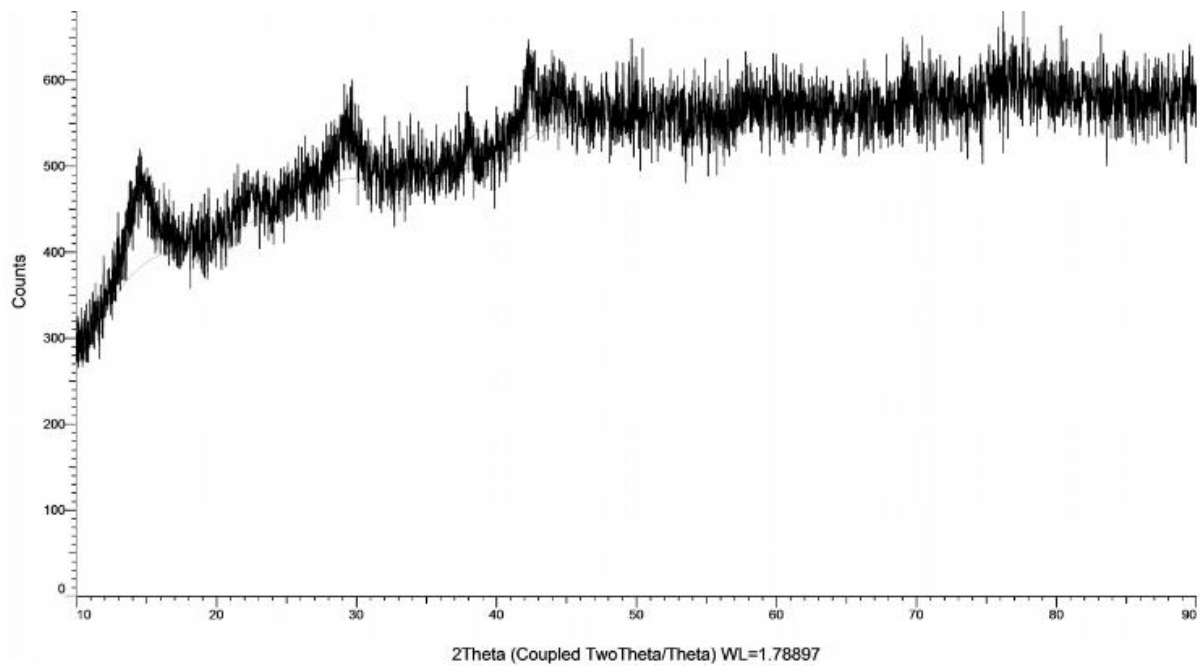


Figure A3. X-ray diffraction pattern of the synthesis of birnessite via KOH (0.9ml min^{-1})

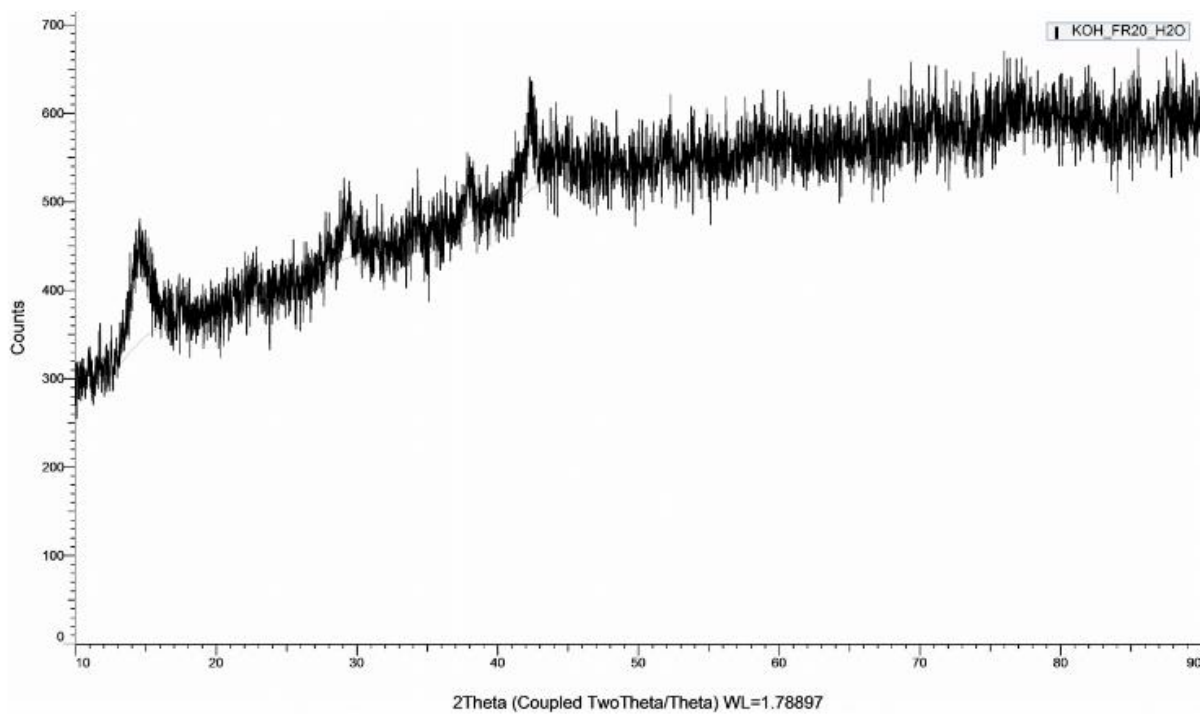


Figure A4. X-ray diffraction pattern of the synthesis of birnessite via KOH (1.7ml min^{-1})

Table 6. Summarised the data of X-ray diffraction for the sample that was synthesized at flow rate 0.22, 0.4 and 0.9 ml min⁻¹

0.4ml/min	Position (θ)	Size (nm)	d-spacing(\AA)
Peak 1	14.493	18.87	7.08409
Peak 2	29.230	23.9	3.54410
0.9ml/min	Position (θ)	Size (nm)	d-spacing(\AA)
Peak 1	14.419	27.85	7.10762
Peak 2	29.106	32.1	3.55133
0.22ml/min	Position (θ)	Size (nm)	d-spacing(\AA)
Peak 1	14.419	27.52	7.1072
Peak 2	29.301	29.82	3.55213